Cell Transplantation, Vol. 26, pp. 805–820, 2017
Printed in the USA.

0963-6897/17 $90.00 + .00
DOI: https://doi.org/10.3727/096368916X694274
E-ISSN 1555-3892
www.cognizantcommunication.com

Precise Regulation of miR-210 Is Critical for the Cellular Homeostasis Maintenance and Transplantation Efficacy Enhancement of Mesenchymal Stem Cells in Acute Liver Failure Therapy

Yingxia Liu,*[1] Yongjia Xiong,†[1] Feiyue Xing,† Hao Gao,‡ Xiaogang Wang,§ Liumin He,† Chaoran Ren,¶ Lei Liu,* Kwok-Fai So,¶ and Jia Xiao*†#

*State Key Discipline of Infectious Diseases, Shenzhen Third People's Hospital, Shenzhen, P.R. China
†Department of Immunobiology, Institute of Tissue Transplantation and Immunology, Jinan University, Guangzhou, P.R. China
‡Institute of Traditional Chinese Medicine and Natural Products, College of Pharmacy, Jinan University, Guangzhou, P.R. China
§Department of Cell Biology and Institute of Biomedicine, Jinan University, Guangzhou, P.R. China
¶Guangdong Medical Key Laboratory of Brain Function and Diseases, GMH Institute of Central Nervous System Regeneration, Jinan University, Guangzhou, P.R. China
#School of Biomedical Sciences, The University of Hong Kong, Hong Kong, P.R. China

Stem cell transplantation is a promising clinical strategy to cure acute liver failure. However, a low cell survival ratio after transplantation significantly impairs its therapeutic efficacy. This is partly due to insufficient resistance of transplanted stem cells to severe oxidative and inflammatory stress at the injury sites. In the current study, we demonstrated that a small molecule zeaxanthin dipalmitate (ZD) could enhance the defensive abilities against adverse stresses of human adipose-derived mesenchymal stem cells (hADMSCs) in vitro and increase their therapeutic outcomes of acute liver failure after transplantation in vivo. Treatment with ZD dramatically improved cell survival and suppressed apoptosis, inflammation, and reactive oxygen species (ROS) production of hADMSCs through the PKC/Raf-1/MAPK/NF-κB pathway to maintain a reasonably high expression level of microRNA-210 (miR-210). The regulation loop between miR-210 and cellular/mitochondrial ROS production was found to be linked by the ROS inhibitor iron–sulfur cluster assembly proteins (ISCU). Pretreatment with ZD and stable knockdown of miR-210 significantly improved and impaired the stem cell transplantation efficacy through the alteration of hepatic cell expansion and injury amelioration, respectively. Vehicle treatment with ZD did not pose any adverse effect on cell homeostasis or healthy animal. In conclusion, elevating endogenous antioxidant level of hADMSCs with ZD significantly enhances their hepatic tissue-repairing capabilities. Maintenance of a physiological level of miR-210 is critical for hADMSC homeostasis.

Key words: Acute liver failure (ALF); Mesenchymal stem cells (MSCs); MicroRNA-210; Zeaxanthin dipalmitate (ZD)

INTRODUCTION

Acute liver failure (ALF) is a kind of fatal liver disease with high mortality and unique difficulty in treatment. Liver transplantation is the only surgical choice for ALF patients. However, severe shortage of donor organs, immunological rejection, surgical complications, and poor prognosis significantly restrict its clinical application[1]. Recently, based on available evidence, stem cell therapy provides a valuable alternative option[2]. After transplantation, naive stem cells or differentiated hepatocyte-like cells rapidly recover essential hepatic functions through replenishing functional hepatocytes and/or evoking endogenous liver regenerative processes via their paracrine actions[3]. However, the therapeutic efficacy of stem cell therapy is impaired by the limitation of viable cells arriving at the injured liver sites, due to an adverse microenvironment caused by severe local inflammation, oxidative stress, and cell death[4,5]. Thus, it is proposed that enhancing the endogenous antioxidant/anti-inflammatory abilities of stem cells before transplantation is beneficial for therapeutic outcomes[5].

Received May 12, 2016; final acceptance January 9, 2017. Online prepub date: December 13, 2016.
[1]These authors provided equal contribution to this work.
Address correspondence to Kwok-Fai So, Ph.D., Guangdong Medical Key Laboratory of Brain Function and Diseases, GMH Institute of Central Nervous System Regeneration, 8th Floor, 2nd Science and Technology Building, Jinan University, Guangzhou 510632, P.R. China. Tel: +86-20-85223563; E-mail: hrmaskf@hku.hk *or* Jia Xiao, Ph.D., State Key Discipline of Infectious Diseases, 8th Floor, Medical Technology Building, Shenzhen Third People's Hospital, Shenzhen 518112, P.R. China. Tel: +86-755-61236314; E-mail: tjxiao@jnu.edu.cn

Zeaxanthin dipalmitate (ZD) is one of the main constituents of the fruit *Lycium barbarum* (wolfberry), which is valued in Chinese culture for nourishing the liver and eyes. We have demonstrated the hepatoprotective properties of wolfberry/ZD in a variety of liver diseases, including alcoholic liver injury[6,7], non-alcoholic fatty liver disease[8,9], and acute liver injury[10]. The alleviation of excessive oxidative stress and promotion of cellular anti-inflammatory activity are the main protective mechanisms of ZD. Since pretreatment with an antioxidant agent (e.g., *N*-acetylcysteine or edaravone) significantly improved the therapeutic efficacy of mesenchymal stem cells (MSCs) in an ALF model, it is pertinent to investigate the molecular mechanisms of ZD in stem cell therapy of liver diseases[5,11].

MicroRNAs (miRNAs) are a class of short noncoding RNAs. Available evidence suggests that the induction of miR-210 is the consistent feature of hypoxic response in both normal and malignant cells[12]. Upregulation of miR-210 inhibits proliferation and induces apoptosis in tumor cells[13]; it is also able to modulate the response of abnormal redox status in normal cells[14] and to protect cells from apoptosis[15]. Importantly, miR-210 ameliorates the hypoxia-induced apoptosis and therefore enhances the survival ratio of stem cells through antioxidative stress processes[16,17].

In this study, we demonstrated that ZD could improve cell viability, reduce apoptosis, and ameliorate inflammation of human adipose-derived mesenchymal stem cells (hADMSCs) induced by lipopolysaccharide and hydrogen peroxide cotreatment (LPS/H_2O_2) through inhibiting the protein kinase C (PKC)/mitogen-activated protein kinase (MAPK)/extracellular signal-regulated kinase (ERK) pathway and balancing the homeostasis of miR-210 expression. The in vivo study also revealed that ZD-pretreated hADMSCs rescued more ALF mice with enhanced therapeutic efficacy via miR-210 regulation.

MATERIALS AND METHODS

Chemicals and Reagents

Pure ZD powder was bought from Carbosynth Limited (Berkshire, UK). Edaravone (3-methyl-1-phenyl-2-pyrazolin-5-one) was purchased from Mitsubishi Pharma Corporation (Tokyo, Japan). Reactive oxygen species (ROS) generator antimycin/rotenone, ROS scavenger *N*-acetyl-L-cysteine (NAC), microRNA-210 (miR-210) mimic (transfection concentration: 20 nM), D-galactosamine (Gal), LPS, and methylthiazolyldiphenyl tetrazolium bromide (MTT) were purchased from Sigma-Aldrich (St. Louis, MO, USA). PD98059 and staurosporine were purchased from Calbiochem (Billerica, MA, USA). All cell culture consumables and reagents were bought from either Corning Incorporated (Corning, NY, USA) or Gibco (Carlsbad, CA, USA). Antibodies against catalase (CAT), superoxide dismutase 1 (SOD1), Raf-1, phosphorylated p38 MAPK at Thr180/Tyr182, total p38 MAPK, phosphorylated MEK at Ser217/221, total MEK, and glyceraldehyde 3-phosphate dehydrogenase (GAPDH) were bought from Cell Signaling (Beverly, MA, USA). H_2O_2 was ordered from Guangzhou Chemical Company (Guangzhou, P.R. China).

Stem Cell Culture and Treatments

hADMSCs were purchased from and validated by Cyagen Biosciences (Guangzhou, P.R. China). Cells were cultured in Dulbecco's modified Eagle's medium (DMEM)/F12 medium (Thermo Fisher Scientific, Waltham, MA, USA) with 10% (v/v) fetal bovine serum (FBS; Thermo Fisher Scientific) at 37°C with 5% CO_2 using a cell incubator (Thermo Fisher Scientific). Before every treatment, cells must reach a confluence of 60%–70%. To induce in vitro oxidative stress and inflammation, cells were incubated with 0.1 μg/ml LPS and 200 μM H_2O_2 simultaneously. This combination of dosages was validated from our previous study[5]. For the pretreatment with ZD, phosphate-buffered saline (PBS; Sigma-Aldrich) with 5% Tween 80 (Sigma-Aldrich) dissolved ZD was added 2 h before the LPS/H_2O_2 treatment. The optimal pretreatment duration was selected on the basis of a previous study and pilot tests[6].

Overexpression and Knockdown Manipulations of miR-210 in hADMSCs by Lentiviral Infection

Genetic manipulations of human cells were approved by the ethical committee of Shenzhen Third People's Hospital. Replication-deficient lentivirus encoding human miR-210 precursor or inhibitor sponge to overexpress (OE) or knock down (KD) the endogenous miR-210 in hADMSCs, respectively, was purchased from Sangong Biotech (Shanghai, P.R. China). Virus without the miR-210 construct was used as control (Ctrl-miR-210). Stem cells (in six-well plates, 3×10^4 cells/well) were transduced with 10 μl of lentiviral vectors with a virus titer of 1×10^8 IFU/ml containing miR-210 precursor or miR-210 inhibitor sponge[18]. After 24 h in complete culture medium, cells were replaced with fresh medium and then left for another 48 h to evaluate the efficiency. Puromycin (0.75 μg/ml; Sigma-Aldrich) was applied to hADMSCs for another 24 h to eliminate the nontransfected cells.

MTT Assay

Stem cell viability was evaluated by the MTT assay. After treatments, cells were washed by sterile PBS thrice and then incubated with 5 mg/ml MTT for 4 h, and subsequently dissolved in dimethyl sulfoxide (DMSO;

Sigma-Aldrich). The absorbance of MTT was measured at 570 nm, and pure DMSO was set as blank.

Calculation of Apoptotic Ratio and Caspase 3/7/8 Activity

The calculation of apoptotic ratio and caspase 3/7/8 activity in hADMSCs were performed as previously described[5,19]. Briefly, after drug treatments, Hoechst 33342 (5 μg/ml) and propidium iodide (PI; 5 μg/ml) were added to stain live cells for 15 min under incubation. The results were expressed as the percentage of apoptosis: PA=apoptotic cell number/total cell number×100%. Activities of caspases 3/7 from cell lysates were measured using Cell Meter Caspase 3/7 Activity Apoptosis Assay Kit (AAT Bio., Sunnyvale, CA, USA) according to the user manual. Results were read at 520 nm in a microplate reader (Bio-Rad, Hercules, CA, USA) and expressed as fold change in caspase 3/7 activity from control.

ROS Production Measurement

Intracellular production of ROS was detected by the staining of 2′,7′-dichlorofluorescin diacetate (DCFH-DA; Sigma-Aldrich). After treatments, cells were washed thrice with sterile PBS and then incubated with 10 μM DCFH-DA for 30 min at 37°C for green fluorescent light visualization. Quantification of the fluorescence was conducted with ImageJ software [Version 1.49; National Institutes of Health (NIH), Bethesda, MD, USA][7].

In Vitro Hepatocyte Differentiation

Cultured hADMSCs at passage 3 were induced to form hepatocytes using a StemXVivo Hepatocyte Differentiation Kit (R&D Systems, Minneapolis, MN, USA) with or without 0.5 μM ZD supplementation. After a 16-day differentiation, the expression of α-fetoprotein (AFP) and hepatocyte nuclear factor 4α (HNF-4α), and the secretion of urea and albumin were examined according to the manufacturer's instructions.

In Vitro Secretion of Hepatocyte Growth Factor (HGF), IL-10, and Indoleamine 2,3-Dioxygenase (IDO) by hADMSCs

To evaluate the secreted levels of HGF, interleukin-10 (IL-10), and IDO by hADMSCs in vitro, medium from cultured cells with or without ZD pretreatment were subjected to corresponding enzyme-linked immunosorbent assay (ELISA) analyses [HGF (RayBiotech, Norcross, GA, USA); IL-10 (PeproTech, Rocky Hill, NJ, USA); IDO (Aviva Systems Biology, San Diego, CA, USA)].

GSH/GSSG Ratio and NF-κB Activity Quantification

The ratio between reduced glutathione (GSH) to oxidized glutathione (GSSG) of each cellular protein sample was measured using a GSH/GSSG detection assay kit from Abcam (Cambridge, UK). The activity of transcription factor nuclear factor (NF)-κB p65 was measured with an NF-κB/p65 ActivELISA kit from Imgenex Corporation (San Diego, CA, USA).

RNA Extraction, cDNA Synthesis, and Quantitative PCR Measurements

Total RNA of cells was extracted using illustra™ RNAspin Mini Kit (GE Healthcare, Pollards Wood, UK). The preparation of the first-strand cDNA was conducted following the instruction of the SuperScript™ First-Strand Synthesis System (Invitrogen, Carlsbad, CA, USA). The mRNA expression levels of epidermal growth factor (EGF) and oncostatin M (OSM) were measured by Takara SYBR Premix Taq Quantitative PCR System (Takara Bio Inc., Shiga, Japan) and a MyiQ2 real-time PCR machine (Bio-Rad). Parallel amplification of GAPDH was used as the internal control. Relative quantification was done using the $2^{-\Delta\Delta Ct}$ method. The relative expression of the specific gene to the internal control was obtained and then expressed as percentage of the control value. All real-time PCR procedures were performed according to the MIQE guideline.

Western Blots

Cells were washed with sterile PBS three times and then subjected to cytosolic and nuclear protein extraction using a NE-PER Nuclear and Cytoplasmic Extraction System (Pierce, Rockford, IL, USA). Protein samples were then quantified with a bicinchoninic acid assay (BCA) method kit from Bio-Rad. Western blot analyses of cell lysates were performed as previously described[10]. Briefly, proteins were diluted and mixed with prepared sample buffer [0.1 M Tris-HCl (pH 6.8), 20% glycerol, 4% sodium dodecyl sulfate (SDS), 0.2% bromophenol blue, and 5.25% β-mercaptoethanol]. The mixture was denatured at 95°C for 5 min followed by electrophoresis in a 10% polyacrylamide gel. The protein was then transferred to an Immun-Blot™ polyvinylidine fluoride (PVDF) membrane (Bio-Rad) in a transfer electrophoresis unit (Bio-Rad). The membrane was then incubated in blocking buffer (5% nonfat milk powder in TBST) for 1 h followed by incubation with appropriate primary antibodies (1:3,000 dilution) in TBST [100 mM Tris-HCl (pH 7.5), 0.9% NaCl, and 0.1% Tween 20] overnight at 4°C with gentle agitation. On the following day, the membrane was washed with TBST and incubated with appropriate secondary antibodies (1:2,000 dilution in TBST) for 2 h at room temperature. After washing off the unbound antibody with TBST, the expression of the antibody-linked protein was determined by an ECL™ Western Blotting Detection Reagent (GE Healthcare). Parallel blotting of GAPDH was used as the internal control.

ALF Mice Model and Treatments

All animal experiments in the current study were approved by and were in accordance with guidelines and regulations from the ethical committees of Jinan University and Shenzhen Third People's Hospital. The ALF model was established as previously described with minor modifications[5]. Briefly, male 6-week-old (~20 g) nonobese diabetic severe combined immunodeficient (NOD/SCID) mice were bought from Guangdong Experimental Animal Center (Guangzhou, P.R. China). Mice were randomly divided into eight groups ($n=12$): (1) control group: mice were intraperitoneally (IP) injected with PBS only; (2) Gal/LPS group: mice were IP injected with 600 mg/kg Gal and 8 μg/kg LPS dissolved in PBS simultaneously; (3–5) vehicle-stem cell groups: mice were injected through the tail vein (t.v.) with 2×10^6 hADMSCs (untreated, 0.5 μM ZD pretreated, or 0.5 μM ZD pretreated miR-210-KD transfected) at passage 3; (6–8) Gal/LPS-stem cell groups: mice received 600 mg/kg Gal and 8 μg/kg LPS via IP injection. Six hours later, mice were injected with 2×10^6 hADMSCs (untreated, 0.5 μM ZD pretreated, or 0.5 μM ZD pretreated miR-210-KD transfected) at passage 3 through t.v. injection. The dosage combination of Gal and LPS, optimal stem cell number for injection, as well as the delivery route of stem cells were selected on the basis of our previous study[5]. Durations of ZD pretreatment and miR-210 knockdown were 24 and 36 h before stem cell transplantation, respectively. Murine sera were collected at days 1, 3, and 7 posttransplantation. Liver samples were collected at the end of the 7-day experiment and stored at −80°C until further processing.

Serum and Liver Tissue Analysis

Serum was collected by centrifugation from whole-blood sample at $1{,}000\times g$ for 10 min at 4°C and stored at −80°C. Liver tissue samples were fixed in 10% phosphate-buffered formalin, processed for histology, and embedded in paraffin blocks. Tissue sections (5 μm) were then cut and stained with hematoxylin and eosin (H&E; Sigma-Aldrich) to exhibit the histological changes. Liver necrosis was calculated by two independent pathologists using ImageJ software quantification.

Serum ALT and AST Assay

To evaluate the hepatic injury at the enzymatic level, serum alanine transaminase (ALT) and aspartate transaminase (AST) levels were measured using ALT (SGPT) and AST (SGOT) reagent sets (Teco Diagnostics, Anaheim, CA, USA) according to the manufacturer's instructions.

Genomic DNA Extraction and Quantitative Real-Time Polymerase Chain Reaction (qRT-PCR)

To quantify the transplanted hADMSCs that homed at the mice liver, a recently established RT-PCR quantification system was used as described in previous studies[5,20]. Briefly, genomic DNA at day 7 posttreatment was extracted from NOD/SCID mouse livers using QIAamp genomic DNA extraction kit (Qiagen, Hilden, Germany). A pair of primers (forward: 5′-ATGCTGATGTCTGGGTAGGG TG-3′; reverse: 5′-TGAGTCAGGAGCCAGCGTATG-3′) that generate a 141-bp fragment of human Down syndrome region at chromosome 21 were used to quantify the human-derived cells.

hADMSC Proliferation and Apoptosis Measurements After Transplantation

Seven days after stem cell transplantation into the injured NOD/SCID mouse liver, donor stem cell proliferation was quantified by immunohistochemical staining of Ki-67 or proliferating cell nuclear antigen (PCNA) with human-specific antibodies (Abcam)[11]. Apoptosis was quantified by terminal dUPT nick-end labeling (TUNEL) using an ApopTag Plus Peroxidase In Situ Apoptosis Detection Kit (Chemicon, Billerica, MA, USA). Sections were costained with human-specific albumin antibodies and Alexa Fluor 488 secondary antibody (Invitrogen). The activity of hepatic tissue caspases 3/7 was measured using Apo-ONE Homogeneous Caspase 3/7 Assay kit (Promega, Madison, WI, USA) according to the user manual. The number of Ki-67$^+$, PCNA$^+$, or TUNEL$^+$ cells was quantified in three microscopic fields at 40× magnification using the ImageJ software.

ELISA Assay

ELISA measurements of secreted/serum tumor necrosis factor-α (TNF-α) and IL-6 were performed using corresponding ELISA development kits from PeproTech according to user instructions. PKC activity ELISA was measured with a PKC kinase activity kit from Enzo Life Sciences (Farmingdale, NY, USA). Change of phosphorylated ETS domain-containing protein (Elk1) at Ser383 was examined using a p-Elk1 colorimetric ELISA kit from ImmunoWay Biotechnology (Newark, DE, USA).

Statistical Analysis

Data from each group were expressed as mean ± standard error of the mean (SEM). Statistical comparison between groups was done using an unpaired *t*-test and a one-way analysis of variance (ANOVA) to detect the difference between two indicated groups. A value of $p<0.05$ was considered to be statistically significant (Prism 5.0; Graphpad software Inc., San Diego, CA, USA).

RESULTS

ZD Potently Ameliorates Cell Injury Induced by LPS and H_2O_2 in hADMSCs

We have confirmed in our previous study that a 24-h incubation with 0.1 μg/ml LPS and 200 μM H_2O_2 induced

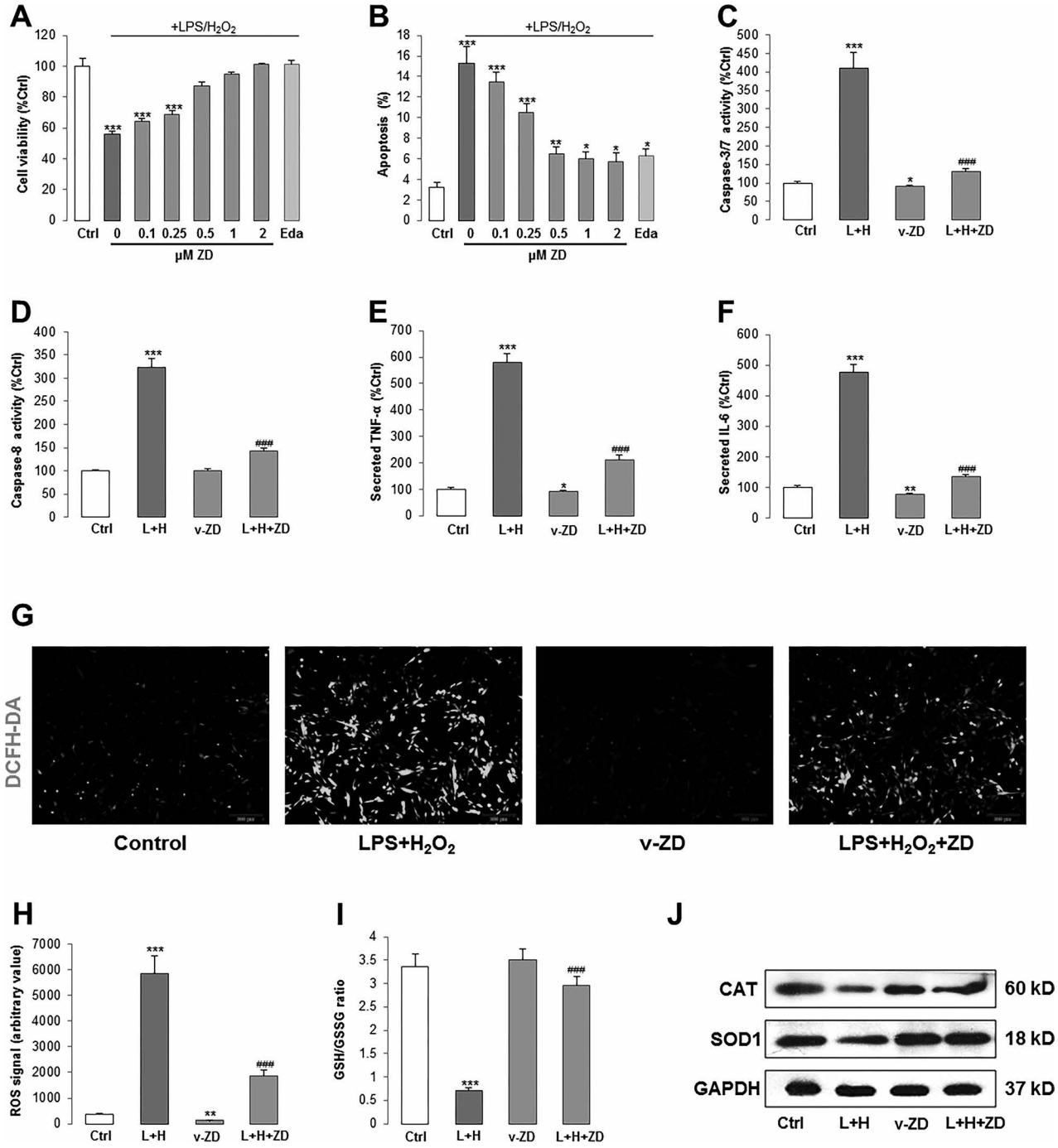

Figure 1. ZD ameliorates cell injury induced by LPS and H_2O_2 in hADMSCs. (A, B) Measurement of cell viability and apoptotic ratio after different doses of ZD (gray column) with or without LPS/H_2O_2 coincubation (dark gray column). A proven stem cell protective agent, edaravone (light gray column), was used as the positive control. (C, D) Activities of caspases 3/7 or caspase 8 from cell lysates after LPS/H_2O_2 incubation with or without ZD cotreatment. (E, F) Secreted TNF-α and IL-6 level changes after LPS/H_2O_2 incubation with or without ZD cotreatment. (G, H) Intracellular production of ROS was detected by fluorescence probe DCFH-DA (200×) after LPS/H_2O_2 incubation with or without ZD cotreatment. (I) Changes of ratio between glutathione (GSH) to oxidized glutathione (GSSG) and (J) Western blot for the expression of CAT and SOD1 after LPS/H_2O_2 incubation with or without ZD cotreatment. The treatment duration is 24 h. *$p<0.05$, **$p<0.01$, ***$p<0.001$ mean significant changes between control and treatments, respectively; ###$p<0.001$ means significant changes between indicated treatment with LPS/H_2O_2 incubation group. L+H, LPS/H_2O_2; Eda, edaravone; v-ZD, vehicle-ZD treatment; Ctrl, control; ZD, zeaxanthin dipalmitate; hADMSCs, human adipose-derived mesenchymal stem cells; LPS, lipopolysaccharide; TNF-α, tumor necrosis factor-α; IL-6, interleukin-6; DCFH-DA, 2′,7′-dichlorofluorescin diacetate; CAT, catalase; SOD1, superoxide dismutase 1; GAPDH, glyceraldehyde 3-phosphate dehydrogenase; ROS, reactive oxygen species.

evident oxidative stress and inflammatory responses in human umbilical cord-derived mesenchymal stem cells (hUC-MSCs)[5]. Thus, in the current study, we used the same treatment conditions to investigate the possible protective properties of ZD in hADMSCs. First, we tried a dose-dependent study of ZD when it was added prior to the stress induction and found that ZD significantly recovered the cell viability damaged by LPS/H_2O_2 from concentrations of 0.5 to 2 μM (Fig. 1A). Consistently, 0.5 to 2 μM ZD pretreatments significantly reduced the cellular apoptotic ratio, which was induced by the stress treatment (from ~15% to ~7%) (Fig. 1B). The protective effects of 0.5 μM ZD on hADMSCs were very similar to those of 10 μM edaravone, an effective clinical antioxidant against oxidative stress and inflammation in hUC-MSCs[5], and we used this dosage of ZD in the following experiment. To further explore the antiapoptotic effects of ZD, we measured the changes of caspases 3/7 and caspase 8 after LPS/H_2O_2 induction with or without ZD pretreatment. The results showed that ZD dramatically reduced the caspases' activities elevated by the stress induction (Fig. 1C and D). Changes of secreted proinflammatory cytokines (TNF-α and IL-6) from hADMSCs further confirmed the anti-inflammatory functions of ZD (Fig. 1E and F).

Then we used DCFH-DA fluorescent dye to test the change of cellular ROS production after stress induction. It was found that LPS/H_2O_2 incubation significantly increased the cellular green fluorescence signals, which were ameliorated by the pretreatment of ZD (Fig. 1G and H). In line with this finding, inhibited GSH/GSSG ratio and CAT/SOD1 protein expressions were also significantly recovered by ZD (Fig. 1I and J). Collectively, our results exhibited potent ameliorative effects of 0.5 μM ZD on cellular oxidative stress and inflammation induced by the LPS/H_2O_2 incubation. Importantly, vehicle-ZD treatment did not cause any change in cell viability (data not shown) but reduced the activity of basal caspases 3/7, level of secreted cytokines, and ROS production, which suggests its health-promoting effect on normal stem cells (Fig. 1C–H).

ZD Rebalanced the PKC/Raf-1/MAPK/NF-κB Pathway and miR-210 Expression Altered by Stress Induction

To further investigate the pathway that mediates the stress induction and ZD protection, we tested the

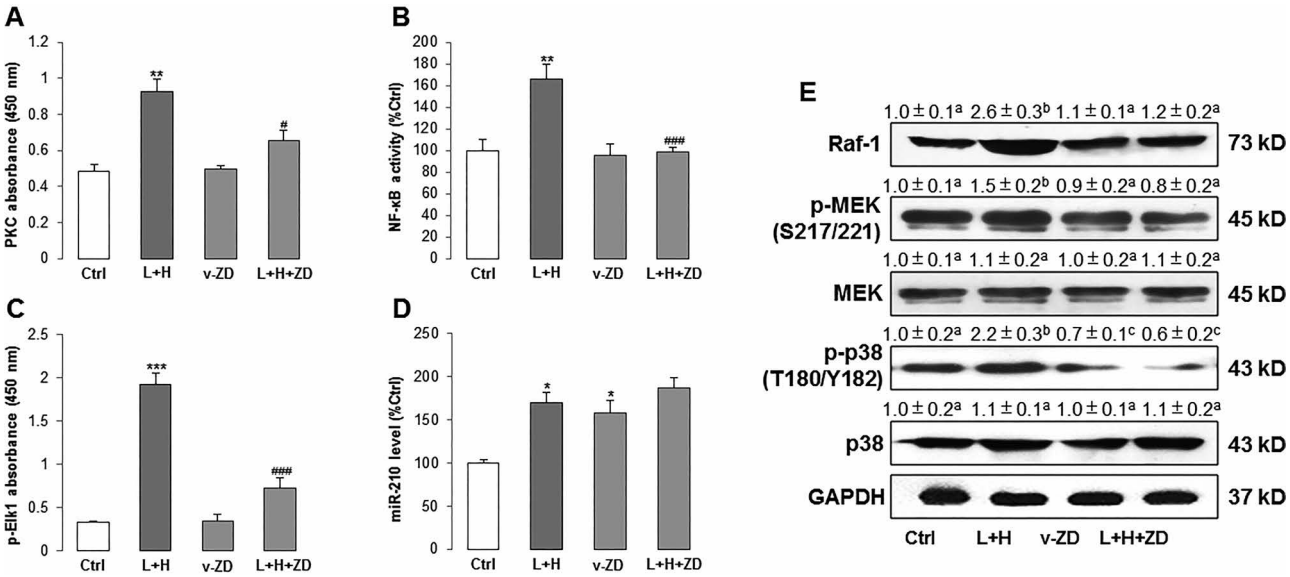

Figure 2. ZD ameliorates PKC/Raf-1/MAPK/NF-κB pathway activity, which was activated by LPS/H_2O_2 in hADMSCs. (A–C) PKC activity, NF-κB (p65), and phosphorylated Elk1 level were measured after LPS/H_2O_2 incubation with or without ZD cotreatment. (D) The expression level of miR-210 was measured after LPS/H_2O_2 incubation with or without ZD cotreatment. (E) Western blot results of Raf-1, phosphorylated MEK, total MEK, phosphorylated p38 MAPK, and total p38 MAPK after LPS/H_2O_2 incubation with or without ZD cotreatment. *$p<0.05$, **$p<0.01$, ***$p<0.001$ mean significant changes between control and treatment groups, respectively; #$p<0.05$, ###$p<0.001$ mean significant changes between indicated treatment and LPS/H_2O_2 incubation group, respectively. (E) Different letters (e.g., a vs. b, b vs. c) indicate a significant change between compared groups ($p<0.05$). The same letters (e.g., a vs. a, c vs. c) indicate there is no significant change between compared groups ($p>0.05$). Ctrl, control; ZD, zeaxanthin dipalmitate; L+H, LPS/H_2O_2; v-ZD, vehicle-ZD treatment; hADMSCs, human adipose-derived mesenchymal stem cells; LPS, lipopolysaccharide; PKC, protein kinase C; NF-κB, nuclear factor κB; Elk1, ETS domain-containing protein; miR-210, microRNA-210; Raf-1, RAF proto-oncogene serine/threonine protein kinase; MEK, mitogen-activated protein kinase; p38, p38 mitogen-activated protein kinase; GAPDH, glyceraldehyde 3-phosphate dehydrogenase.

PKC/Raf-1/MAPK/NF-κB pathway since it was reported by other studies to regulate stem cell oxidative stress and inflammatory responses[21–23]. LPS/H_2O_2 incubation significantly increased the activity of PKC, NF-κB (p65), and phosphorylated level of Elk1 in hADMSCs. Pretreatment with ZD either fully or partly abolished such effects without influencing their basal levels (Fig. 2A–C). We then investigated the expressional change of miR-210. In agreement with previous studies[14–16], when compared with the control group, induction of oxidative stress and inflammation in hADMSCs significantly increased the expression of miR-210 (~1.7-fold). Treatment with vehicle-ZD also induced its overexpression (~1.6-fold) but did not further enhance the elevation from stress incubation (from ~1.7-fold to ~1.8-fold) (Fig. 2D). In addition, Raf-1 and MAPK family members (phosphorylated MEK and p38 MAPK) were also activated by LPS/H_2O_2 incubation but were downregulated by ZD pretreatment. The total expression levels of MEK and p38 MAPK, however, were not altered by those treatments (Fig. 2E).

To further prove the involvement of the PKC/Raf-1/MAPK/NF-κB pathway in LPS/H_2O_2-induced stem cell damage and miR-210 expressional alteration, we used the pharmacological inhibitor of PKC (staurosporine) or MEK/MAPK (PD98059) with LPS/H_2O_2/ZD treatments. We found that the inhibition of PKC or MEK/MAPK caused a significant decrease in cell survival and an increase in apoptosis of ZD-treated hADMSCs, when compared with uninhibited ZD-treated hADMSCs (Fig. 3A and B). Furthermore, PD98059 or staurosporine impaired the ameliorated effect of ZD on the secretion level of TNF-α, which represented the cellular inflammatory response level (Fig. 3C). For miR-210, its elevated expression by LPS/H_2O_2 and/or ZD was significantly

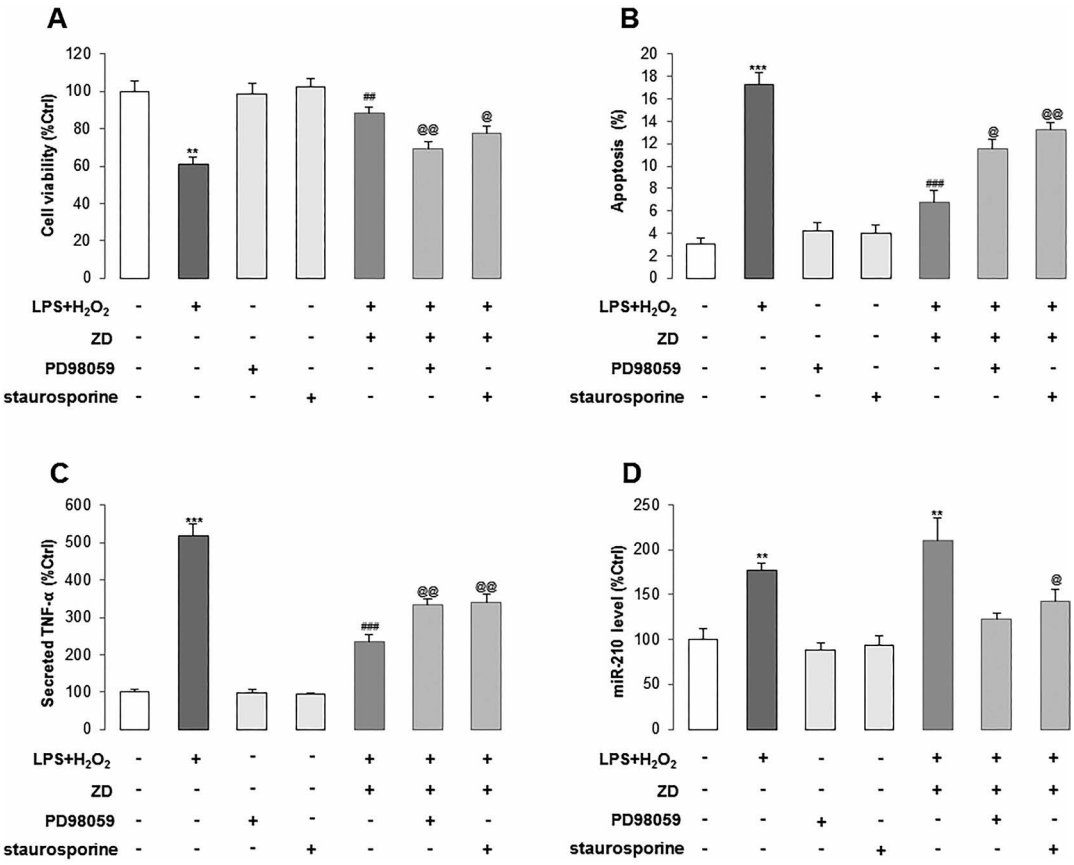

Figure 3. ZD improves stress-induced cell damage and the level of miR-210 through the PKC/MAPK pathway in hADMSCs. (A–D) Cell viability, apoptotic ratio, secretion of TNF-α, and miR-210 expression were measured after LPS/H_2O_2 incubation with or without ZD cotreatment, MAPK inhibitor PD98059, or PKC inhibitor staurosporine. White column: control group, dark gray column: LPS/H_2O_2 coincubation group, light gray column: vehicle-PD98059 or vehicle-staurosporine group, gray column: LPS/H_2O_2+ZD, PD98059, or staurosporine group. $^{**}p<0.01$, $^{***}p<0.001$ mean significant changes between control and treatment groups, respectively; $\#\#p<0.01$, $\#\#\#p<0.001$ mean significant changes between indicated treatment and LPS/H_2O_2 incubation group, respectively; $@p<0.05$, $@@p<0.01$ mean significant changes between LPS/H_2O_2+ZD group and LPS/H_2O_2+ZD+PD98059 or LPS/H_2O_2+ZD+staurosporine groups, respectively. ZD, zeaxanthin dipalmitate; hADMSCs, human adipose-derived mesenchymal stem cells; LPS, lipopolysaccharide; TNF-α, tumor necrosis factor-α; miR-210, microRNA-210.

inhibited by the addition of PD98059 or staurosporine, indicating that both PKC and MEK/MAPK were responsible for the activation of miR-210 after stress induction and ZD protection (Fig. 3D). Vehicle treatment with PD98059 or staurosporine did not influence the basal level of cell viability, apoptosis, TNF-α secretion, and miR-210 expression.

Positive Feedback Loop Between ROS Generation and miR-210 via ISCU1/2

Since ZD inhibited the ROS generation via regulating the PKC/Raf-1/MAPK/NF-κB pathway without potently influencing the miR-210 expression, it is necessary to investigate the relationship between ROS generation and miR-210 expression. We first used different concentrations of ROS generator antimycin (5, 10, and 100 nM) or rotenone (5, 10, and 100 pM) to treat hADMSCs for 24 h and found that 10 nM antimycin and 10 pM rotenone induced the highest expression level of miR-210 (Fig. 4A). Then we used these two concentrations to perform a time-lapse study, and it was demonstrated that 24 h was the optimal treatment duration (Fig. 4B). Antimycin-, rotenone-, or LPS/H_2O_2-induced expression of miR-210 was attenuated by the ROS scavenger NAC coincubation, suggesting that LPS/H_2O_2-increased miR-210 expression is primarily mediated by ROS generation (Fig. 4C). Interestingly, cotreatment with ZD significantly increased the basal miR-210 expression (to approximately twofold of the control level) but attenuated the overexpression of miR-210 induced by antimycin or rotenone (from four- to fivefold to approximately threefold of the control level), indicating that ZD was able to maintain a relatively high level of miR-210 expression in hADMSCs, both under normal and stress conditions (Fig. 4D). It should be noted that NAC could partially reverse the inductive effect of ZD on basal miR-210 expression (Fig. 4D).

To look at the effects of miR-210 expression on ROS generation, we then treated hADMSCs with the miR-210 mimic with or without ZD and found that the miR-210

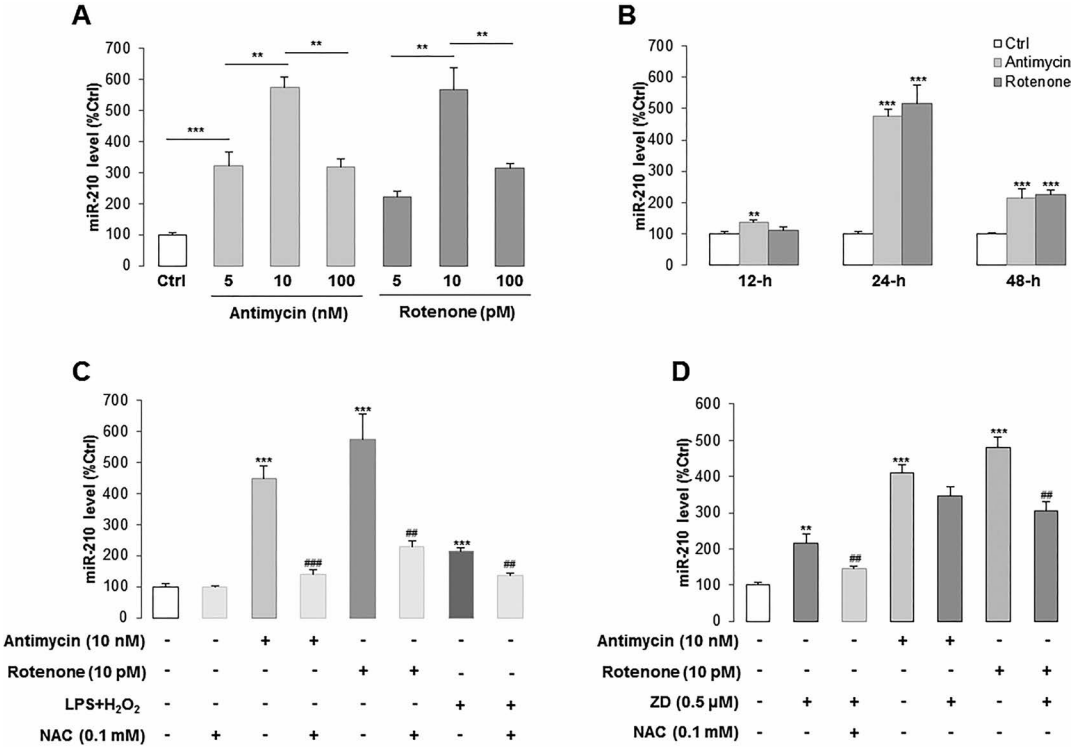

Figure 4. The expression level of miR-210 in hADMSCs is directly regulated by cellular ROS production and ZD treatment. (A, B) The expression of miR-210 was dose-dependently induced by ROS generator antimycin or rotenone after different incubation durations. (C) miR-210 expression was measured in hADMSCs when treated with antimycin, rotenone, LPS/H_2O_2 with or without NAC, a kind of ROS scavenger. (D) ZD cotreatment successfully reduced the elevated miR-210 expression by antimycin or rotenone. $^{**}p<0.01$, $^{***}p<0.001$ mean significant changes between control and treatment groups, respectively; $^{\#\#}p<0.01$, $^{\#\#\#}p<0.001$ mean significant changes between added NAC and non-added NAC group or between nontreated and treated with ZD group, respectively. Ctrl, control; ZD, zeaxanthin dipalmitate; hADMSCs, human adipose-derived mesenchymal stem cells; LPS, lipopolysaccharide; NAC, *N*-acetyl-L-cysteine; miR-210, microRNA-210.

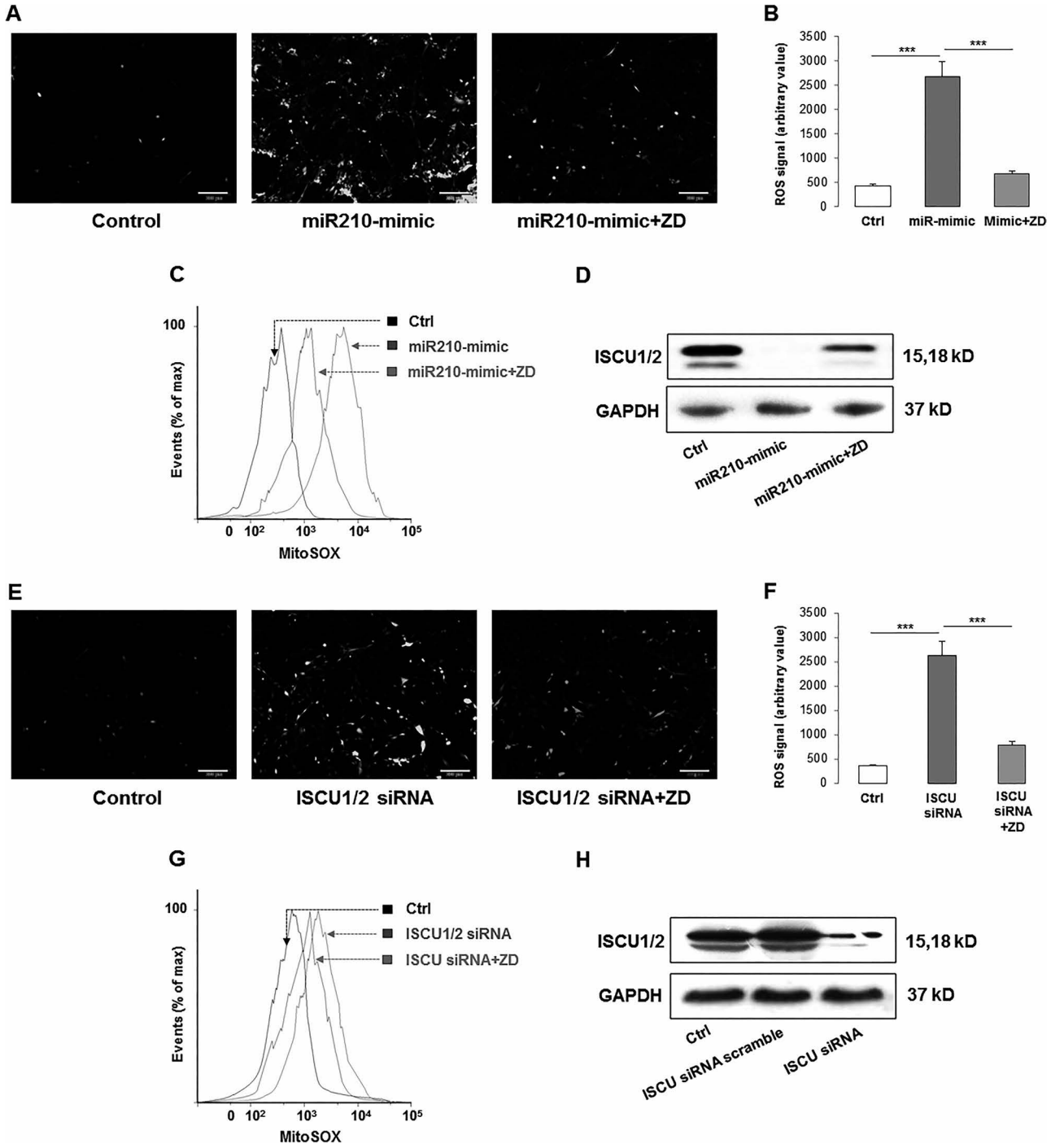

Figure 5. Cross-regulation between miR-210 and cellular ROS generation through ISCU1/2 in hADMSCs. (A–C) miR-210 mimic induced the generation of cellular and mitochondrial ROS, while ZD ameliorated the increase of those ROS productions. (D) After miR-210 mimic treatment, the production of ISCU was significantly decreased, while ZD recovered it. (E–H) When ISCU was knocked down by specific siRNA, both cellular and mitochondrial ROS were induced but inhibited by the ZD cotreatment. (C) and (G) Higher MitoSOX readout means more severe accumulation of mitochondrial ROS. ***$p < 0.001$ means significant change between indicated treatment groups. Ctrl, control; ZD, zeaxanthin dipalmitate; ROS, reactive oxygen species; miR-210, microRNA-210; mitoSOX, mitochondrial superoxide indicator; ISCU1/2, iron–sulfur cluster assembly proteins 1/2; siRNA, small interfering RNA; GAPDH, glyceraldehyde 3-phosphate dehydrogenase.

mimic itself was capable of increasing the ROS generation in cells. Cotreatment with ZD significantly reduced ROS production to a control-comparable level (Fig. 5A and B). Then we measured mitochondrial ROS (MitoSOX) in hADMSCs with the same treatment conditions, and the results corresponded to previous observations, that is, the miR-210 mimic significantly induced the accumulation of mitochondrial ROS while ZD ameliorated this phenomenon (Fig. 5C). To further investigate the effects of miR-210 expression on ROS generation, we measured the expression of the ROS inhibitor iron–sulfur cluster assembly proteins 1/2 (ISCU1/2) in hADMSCs treated with the miR-210 mimic with or without ZD and found that the expression of ISCU1/2 was inhibited by the miR-210 mimic but recovered by ZD cotreatment (Fig. 5D). When ISCU1/2 expression was knocked down by its specific siRNA, both total and mitochondrial ROS productions were significantly increased. Coincubation with ZD significantly ameliorated that effect (Fig. 5E–G).

Then we constructed replication-deficient lentivirus-encoding human miR-210 precursor or inhibitor sponge to OE or KD the endogenous expression of miR-210 in hADMSCs, respectively (Fig. 6A). We found that miR-210 overexpression had no significant effect on cell

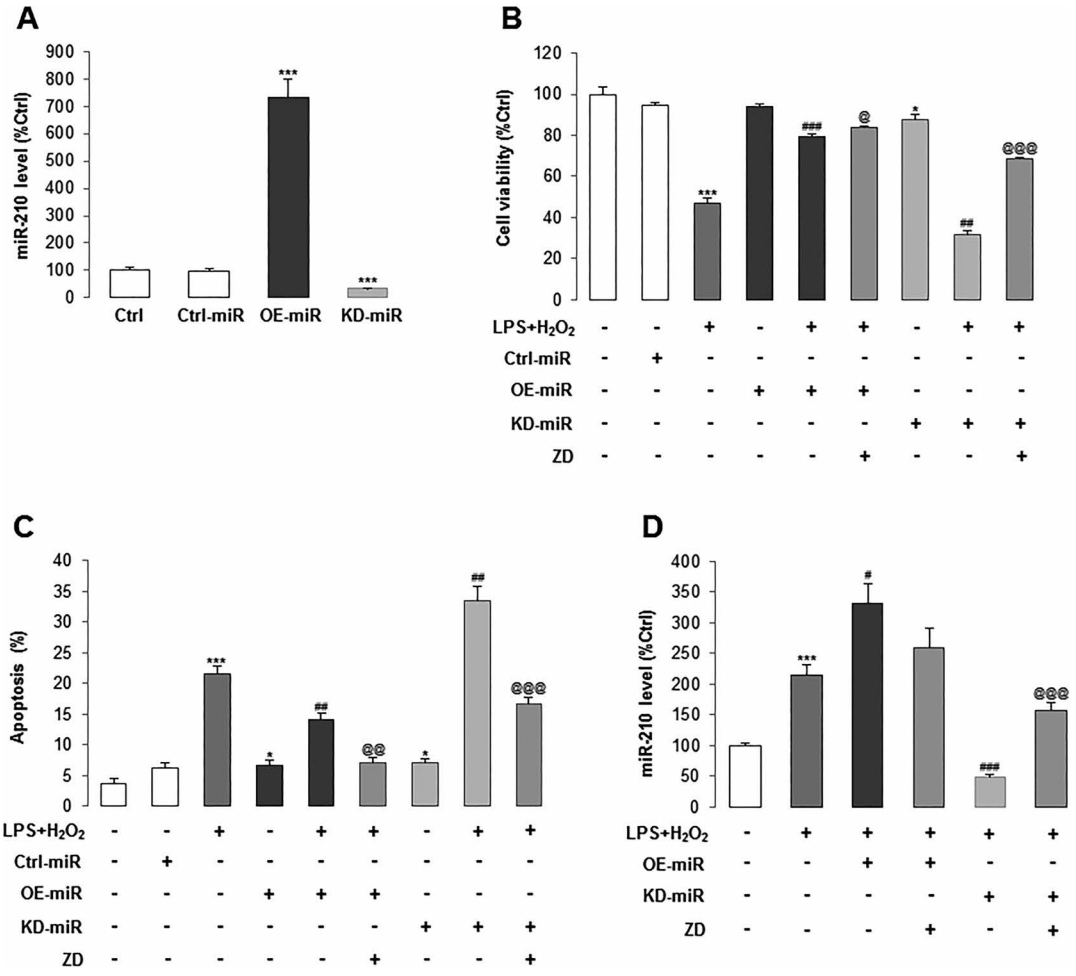

Figure 6. Maintenance of normal miR-210 expression is critical for cell homeostasis of hADMSCs. (A) We constructed replication-deficient lentivirus-encoding human miR-210 precursor or inhibitor sponge to overexpress (OE) or knock down (KD) the endogenous expression of miR-210 in hADMSCs, respectively. (B, C) Cell viability and apoptotic ratio were measured after OE or KD of miR-210 in stem cell pretreated with LPS/H_2O_2 or not, in the absence or presence of ZD. (D) Treated OE or KD of miR-210 in stem cell with LPS/H_2O_2 with or without ZD altered the level of miR-210. Dark gray column: LPS/H_2O_2 coincubation, dark columns: overexpressed miR-210 with or without LPS/H_2O_2 treatment, gray columns: LPS/H_2O_2 + overexpressed miR-210 + ZD cotreatment, light gray columns: knocked down miR-210 with or without LPS/H_2O_2 treatment. $*p<0.05$, $**p<0.001$ mean significant changes between control and indicated treatment groups, respectively; $\#p<0.05$, $\#\#p<0.01$, $\#\#\#p<0.001$ mean significant changes between LPS/H_2O_2 treatment group and OE/KD miR-210 group, respectively; $@p<0.05$, $@@p<0.01$, $@@@p<0.001$ mean significant change between non-treated and treated with ZD group, respectively. Ctrl, control; miR, microRNA; LPS, lipopolysaccharide; ZD, zeaxanthin dipalmitate; hADMSCs, human adipose-derived mesenchymal stem cells.

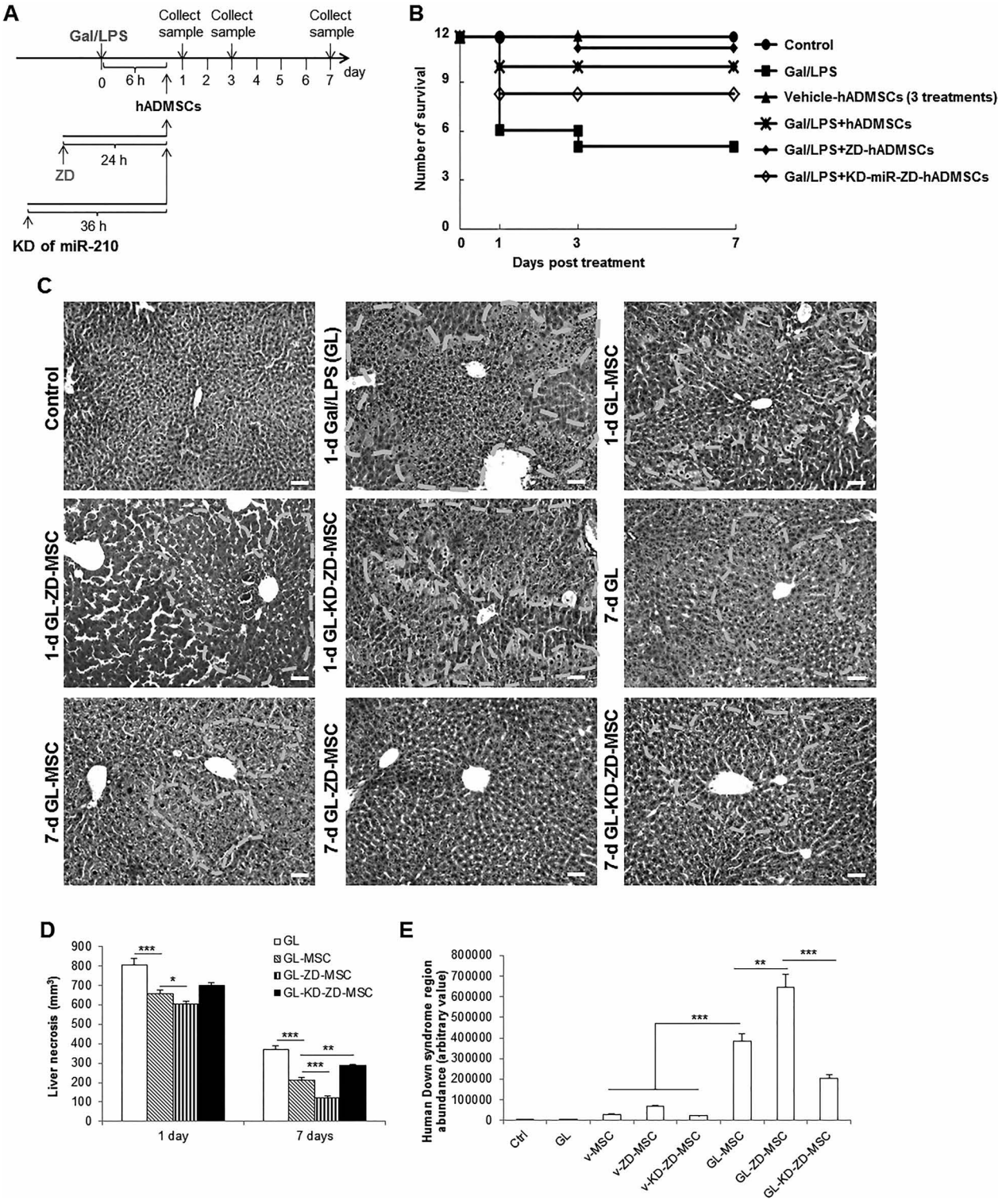

Figure 7. ZD significantly increased and stable knockdown of miR-210 impaired the therapeutic efficacy of transplanted hADMSCs in a murine ALF model, respectively. (A) Mice survival numbers were recorded for 7 days with indicated treatments. (B, C) Representative hepatic H&E images (200×) and corresponding liver necrosis quantification of mice at day 1 and day 7 that received indicated treatments. White dashed line defined areas that are typical necrotic and inflammatory sites in the liver. (D) Expanded cell number in the host mice liver after stem cell transplantation. *$p<0.05$, **$p<0.01$, ***$p<0.001$ mean significant changes between indicated groups, respectively. Ctrl, control; GL, Gal/LPS cotreatment; hADMSCs, human adipose-derived mesenchymal stem cells; KD, stable knockdown of miR-210; Gal, galactosamine; LPS, lipopolysaccharide; miR-210, microRNA-210; v-, vehicle-.

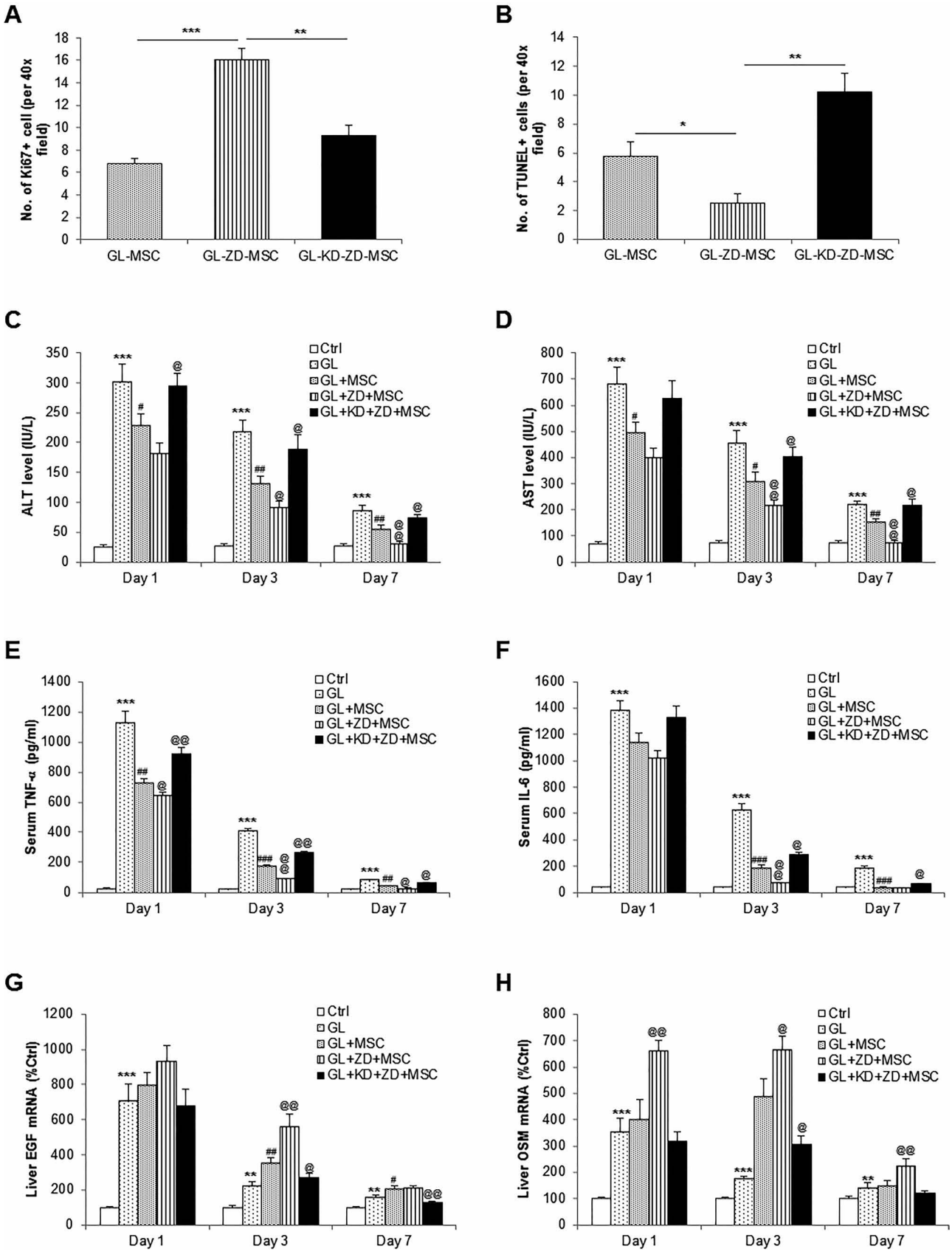
A
No. of Ki67+ cell (per 40x field)
GL-MSC
GL-ZD-MSC
GL-KD-ZD-MSC
B
No. of TUNEL+ cells (per 40x field)
C
ALT level (IU/L)
D
AST level (IU/L)
E
Serum TNF-α (pg/ml)
F
Serum IL-6 (pg/ml)
G
Liver EGF mRNA (%Ctrl)
H
Liver OSM mRNA (%Ctrl)
Ctrl
GL
GL+MSC
GL+ZD+MSC
GL+KD+ZD+MSC
Day 1
Day 3
Day 7

viability and apoptotic ratio but significantly recovered the impaired cell viability and ameliorated the apoptosis induced by LPS/H_2O_2. In contrast, miR-210 KD significantly reduced the basal cell viability and aggravated the damaging effects from LPS/H_2O_2. Apoptotic ratio changes exhibited similar results (Fig. 6B and C). These suggested that a basal level of miR-210 is important for the cell function maintenance. We also tested the function of miR-210-KD cells treated with LPS/H_2O_2 with or without ZD and found that cotreatment with ZD significantly recovered the cell viability damaged by LPS/H_2O_2 and significantly reduced the cellular apoptotic ratio that was induced by the stress treatment (Fig. 6B and C). It corresponded to a previous observation that ZD was able to maintain a relatively high level of miR-210 expression in hADMSCs, regardless of whether miR-210 was endogenously inhibited. In addition, overexpression of miR-210 further enhanced its expression after the challenge of LPS/H_2O_2, while ZD could only slightly reduce the expression. However, ZD pretreatment significantly recovered the miR-210 expression, which was downregulated by its lentiviral inhibition (Fig. 6D).

ZD Promoted Hepatocyte Differentiation Efficiency and Immune-Regulatory Function of hADMSCs

As an important mechanism to exert the tissue-repairing function in the liver, after successful homing, stem cells must undergo hepatocyte differentiation to replenish damaged host hepatocytes. Thus, we investigated the possible promotive effects of ZD on hADMSC hepatocyte differentiation. The results found that the addition of ZD in the differentiation medium enhanced the expression level of key hepatocyte-produced proteins (AFP and HNF4) and the secreted level of urea and albumin when compared with no ZD supplement control (Supplementary Fig. 1A and B; the supplementary figure is available at https://www.dropbox.com/s/jbj3qeu5jtrf6x3/Supplementary%20Figure%201.tif?dl=0). In addition, 24-h incubation with ZD enhanced the secretion of several immune-regulatory mediators, including HGF, IL-10, and IDO from hADMSCs (Supplementary Fig. 1C). Taken together, ZD promoted hepatocyte differentiation efficiency and immune-regulatory function of hADMSCs in vitro.

ZD Enhanced the Engraftment and Survival-Promoting Efficacy of hADMSCs in an ALF Model

Seven days after the Gal/LPS-induced ALF in NOD/SCID mice (Fig. 7A), only 5 mice out of 12 survived. For those mice that received coinjection of hADMSCs, the survival number increased from 5 to 10. ZD-treated stem cells further rescued 1 mouse (from 10 to 11). In the transplanted group of miR-210-KD and ZD-treated hADMSCs after Gal/LPS intoxication, 4 mice out of 12 died during the experiment (Fig. 7B). Vehicle injection of stem cells (naive or miR-210-KD) did not cause any death of mice.

Gal/LPS treatment is known to induce severe necrosis and inflammation of the liver. In the current study, Gal/LPS treatment alone caused evident hepatic necrosis in the NOD/SCID mice within 24 h (Fig. 7C). Administration of naive hADMSCs significantly alleviated such hepatic injury (Fig. 7C and D). However, administration of ZD-pretreated miR-210-KD hADMSCs showed only minimal therapeutic effects when compared to the non-stem cell-injected Gal/LPS group (Fig. 7C and D). Seven days after the treatment, ZD-pretreated naive stem cells showed the best ameliorative effects, while ZD-pretreated miR-210-KD stem cells exhibited worse therapeutic effects (Fig. 7C and D).

To quantify the stem cell engraftments in the NOD/SCID mice liver, the ratio between human gene (Down syndrome region sequence) and host genome at the end of the experiment (day 7) was determined using qRT-PCR. It was found that vehicle stem cell groups (including naive, ZD pretreated, and ZD, pretreated miR-210-KD cells) only generated a small amount of human gene (Fig. 7E). Transplantation with ZD-pretreated hADMSCs following the Gal/LPS intoxication showed the highest abundance of human gene, while ZD-pretreated miR-210-KD hADMSCs showed significantly less human gene copies than that of naive hADMSCs after Gal/LPS intoxication (Fig. 7E). These results suggested that

FACING PAGE

Figure 8. Therapeutic effects of transplanted hADMSCs in a murine ALF model were significantly increased by ZD pretreatment and impaired by stable knockdown of cellular miR-210 expression, respectively. Changes in (A) hepatic Ki-67$^+$ cells, (B) hepatic TUNEL$^+$ cells, (C) serum ALT level, (D) serum AST level, (E) serum TNF-α level, (F) serum IL-6 level, (G) hepatic EGF mRNA, and (H) hepatic OSM mRNA at day 7 of mice after indicated treatments. *$p<0.05$, **$p<0.01$, ***$p<0.001$ mean significant changes between control and indicated treatment groups, respectively; #$p<0.05$, ##$p<0.01$, ###$p<0.001$ mean significant changes between transplanted hADMSC treatment group and nontransplanted group, respectively; @$p<0.05$, @@$p<0.01$, @@@$p<0.001$ mean significant change between nontreated group and treated with ZD or miR-210-KD treated with ZD, respectively. Ctrl, control; GL, Gal/LPS cotreatment; hADMSCs, human adipose-derived mesenchymal stem cells; KD, stable knockdown of miR-210; Gal, galactosamine; LPS, lipopolysaccharide; miR-210, microRNA-210; v-, vehicle-; Ki-67, antigen Ki-67; TUNEL, terminal deoxynucleotidyl transferase dUTP nick-end labeling; ALT, alanine transaminase; AST, aspartate transaminase; TNF, tumor necrosis factor; IL-6, interleukin-6; EGF, epidermal growth factor; OSM, oncostatin M.

administration of hADMSCs after acute liver injury could accelerate the host hepatic regenerative process, and ZD pretreatment significantly improved while miR-210-KD impaired these effects.

To examine the influence of antioxidant status in stem cell proliferation and apoptosis after transplantation, we quantified the number of Ki-67$^+$, PCNA$^+$, or apoptotic cells (with costaining of hCK-18) per 40× high-powered field. It was shown that, when compared with naive and miR-210-KD hADMSCs, pretreatment with ZD significantly increased the Ki-67$^+$ or PCNA$^+$ cell number but reduced the apoptotic cell number, indicating a potentiated resistance of ZD incubation against host liver stresses (Fig. 8A and B, Supplementary Fig. 2A; the supplementary figure is available at https://www.dropbox.com/home/CT-1625%20accepted%20version?preview=Supplementary+Figure+2.tif). Change of hepatic tissue caspase 3/7 activity confirmed this finding (Supplementary Fig. 2B). To further study the influence of ZD and miR-210-KD on the therapeutic effects of hADMSCs, changes in serum ALT and AST levels in each group of mice were evaluated at 1, 3, and 7 days postinjection of the Gal/LPS challenge. One and 3 days after the Gal/LPS challenge, both the ALT and AST levels in the serum of all Gal/LPS-treated mice increased significantly compared to those of the untreated control mice. Transplantation with hADMSCs significantly reduced the serum aminotransferase concentrations, while pretreatment with ZD or miR-210-KD further improved or aggravated such effects, respectively (Fig. 8C and D). This result was supported by the changes in serum inflammatory markers TNF-α and IL-6 (Fig. 8E and F). Last, we measured the hepatic expressional changes of liver regeneration-related genes, OSM and EGF, in the mice liver at days 1, 3, and 7 posttreatment. At days 1 and 3, treatment with Gal/LPS significantly induced the expression of these two genes, which was further enhanced by the injection with hADMSCs. As expected, ZD further enhanced the expression, while miR-210-KD reduced it (Fig. 8G and H). At day 7, the expressional changes of these genes were not as obvious as those of day 1 or 3.

DISCUSSION

Liver transplantation is the most effective strategy for ALF therapy. However, severe shortage of donor organs, surgical complications, immunological rejection, and high medical costs significantly limited its application in the clinic, which forced clinicians and scientists to explore the feasibility of alternatives such as cell therapy. Stem cell-based therapy has been recognized as a promising candidate, although its efficacy is still below expectation in most cases[24,25]. One major problem of the clinical application of stem cell-based therapy is the poor cell viability because of the harsh oxidative stress and inflammatory environment of injured tissue[26]. To date, several antioxidants, including NAC, edaravone, and melatonin, have been shown to safely increase transplantation efficacy through enhancing the endogenous defending ability against oxidative stress, inflammation, apoptosis, and other stresses[5,26–28]. This strategy also avoids possible carcinogenic risk evoked by genetic manipulation of the stem cell[29]. Thus, it is important to discover more small molecules, particularly those from natural products with potent ameliorative functions and minimal side effects, for the optimal treatment before stem cell transplantation.

ZD is the major component (>65% of weight) of carotenoids from wolfberry[30]. Its antioxidant property has been characterized in several disease models. Here we demonstrated that as an antioxidant, ZD drastically increased the endogenous antioxidant abilities of stem cells when under stress environments both in vitro and in vivo. At the concentration of 0.5 μM, ZD has the highest ability to increase the survival ratio and decrease the apoptosis of hADMSCs, which was much lower than the effective concentration of edaravone (10 μM)[5]. Additionally, vehicle treatment with ZD did not pose any adverse effect on cell homeostasis and healthy animal (data not shown), suggesting that ZD is a safe agent in enhancing stem cell therapy efficacy.

Previous studies have proved the key roles of MAPK pathway in stress-induced stem cell damage[5,11]. However, other involved pathways still need exploration. Here we exhibited that miR-210 was a critical molecule for the (1) mediation of the endogenous antioxidant ability and (2) maintenance of the cell homeostasis when it was kept within a reasonably high-level range. When exogenous stress (e.g., oxidative stress and inflammation) occurred, the PKC/Raf-1/MAPK/NF-κB pathway was activated to increase the expression of miR-210. Through ISCU1/2 regulation, treatment with antioxidant (e.g., ZD) was also capable of tuning the miR-210 expression within that range to inhibit the excessive production of cellular ROS. This result is consistent with recent reports that a controllable level of miR-210 can enhance stem cell survival and reduce cell apoptosis under hypoxic or high-oxidative conditions[16,17]. Most importantly, our data suggested the key role of the precise regulation of hepatic miR-210 expression in stem cell homeostasis maintenance and its transplantation efficacy enhancement. Under stress conditions, stem cell miR-210 expression was spontaneously induced to keep normal cell functions. Exogenous antioxidant (e.g., ZD in the current study) agent helped to induce miR-210 upregulation (~1.6-fold) and reduce basal responses of inflammation, apoptosis, and oxidative stress in stem cells (Fig. 1), indicating that ZD itself had an impact already on the stem cells to change their biological features as well as maintain a reasonable cellular miR-210 concentration to facilitate such defensive

mechanism. In addition, since knockdown of endogenous miR-210 expression impaired stem cell viability and induced apoptosis, while overexpression of miR-210 counteracted the damaging effects from exogenous toxin incubation (Fig. 6), it seemed that elevation of basal miR-210 expression in stem cells by vehicle-ZD treatment was the direct reason of improved cell conditions exhibited in Figure 1. Indeed, this conclusion and functions of other related pathways reported by recent studies, such as c-Met, protein tyrosine phosphatase, non-receptor type 2 (PTPN2), and Bcl-2 adenovirus E1B 19 kDa-interacting protein 3 (BNIP3), still warrant investigation[15,21,31].

It is becoming clear that a fine-tuning regulation of ROS is vital for high efficacious stem cell therapies[31]. As oxidative stress, inflammation, and necroapoptosis are typical consequences of ALF, transplantation with enhanced antioxidative ability of stem cells may significantly improve the therapeutic outcomes in clinical trials. Furthermore, as a potent and safe natural product-derived small molecule, ZD could be a promising antioxidant during stem cell preparation.

ACKNOWLEDGEMENTS: This study was supported by Major Science and Technology Projects of Guangdong Province (No. 2015B020225005), Basic Research Fund of Shenzhen City (No. JCYJ20150402111430633), National Natural Science Foundation of China (Nos. 31300813, 81370971, and 81570552), Key Basic Study and Functional Product Research of Wolfberry Grant from Ningxia Province (to J. Xiao and K.-F. So), and Guangdong Natural Science Funds for Distinguished Young Scholar (No. S2013050013880). The authors declare no conflicts of interest.

REFERENCE

1. Mendizabal M, Silva MO. Liver transplantation in acute liver failure: A challenging scenario. World J Gastroenterol. 2016;22:1523–31.
2. Wesson RN, Cameron AM. Stem cells in acute liver failure. Adv Surg. 2011;45:117–30.
3. Zhang Z, Wang FS. Stem cell therapies for liver failure and cirrhosis. J Hepatol. 2013;59:183–5.
4. Dernbach E, Urbich C, Brandes RP, Hofmann WK, Zeiher AM, Dimmeler S. Antioxidative stress-associated genes in circulating progenitor cells: Evidence for enhanced resistance against oxidative stress. Blood 2004;104:3591–7.
5. Zeng W, Xiao J, Zheng G, Xing F, Tipoe GL, Wang X, He C, Chen ZY, Li Y. Antioxidant treatment enhances human mesenchymal stem cell anti-stress ability and therapeutic efficacy in an acute liver failure model. Sci Rep. 2015;5:11100.
6. Xiao J, Wang J, Xing F, Han T, Jiao R, Liong EC, Fung ML, So KF, Tipoe GL. Zeaxanthin dipalmitate therapeutically improves hepatic functions in an alcoholic fatty liver disease model through modulating MAPK pathway. PLoS One 2014;9:e95214.
7. Xiao J, Zhu Y, Liu Y, Tipoe GL, Xing F, So KF. Lycium barbarum polysaccharide attenuates alcoholic cellular injury through TXNIP-NLRP3 inflammasome pathway. Int J Biol Macromol. 2014;69:73–8.
8. Xiao J, Liong EC, Ching YP, Chang RC, Fung ML, Xu AM, So KF, Tipoe GL. Lycium barbarum polysaccharides protect rat liver from non-alcoholic steatohepatitis-induced injury. Nutr Diabetes 2013;3:e81.
9. Xiao J, Xing F, Huo J, Fung ML, Liong EC, Ching YP, Xu A, Chang RC, So KF, Tipoe GL. Lycium barbarum polysaccharides therapeutically improve hepatic functions in non-alcoholic steatohepatitis rats and cellular steatosis model. Sci Rep. 2014;4:5587.
10. Xiao J, Liong EC, Ching YP, Chang RC, So KF, Fung ML, Tipoe GL. Lycium barbarum polysaccharides protect mice liver from carbon tetrachloride-induced oxidative stress and necroinflammation. J Ethnopharmacol. 2012; 139:462–70.
11. Drowley L, Okada M, Beckman S, Vella J, Keller B, Tobita K, Huard J. Cellular antioxidant levels influence muscle stem cell therapy. Mol Ther. 2010;18:1865–73.
12. Chan YC, Banerjee J, Choi SY, Sen CK. miR-210: The master hypoxamir. Microcirculation 2012;19:215–23.
13. Hong L, Han Y, Zhang H, Zhao Q, Qiao Y. miR-210: A therapeutic target in cancer. Expert Opin Ther Targets 2013;17:21–8.
14. Fasanaro P, D'Alessandra Y, Di Stefano V, Melchionna R, Romani S, Pompilio G, Capogrossi MC, Martelli F. MicroRNA-210 modulates endothelial cell response to hypoxia and inhibits the receptor tyrosine kinase ligand Ephrin-A3. J Biol Chem. 2008;283:15878–83.
15. Wang F, Xiong L, Huang X, Zhao T, Wu LY, Liu ZH, Ding X, Liu S, Wu Y, Zhao Y, Wu K, Zhu LL, Fan M. miR-210 suppresses BNIP3 to protect against the apoptosis of neural progenitor cells. Stem Cell Res. 2013;11:657–67.
16. Qiu Y, Chen Y, Zeng T, Guo W, Zhou W, Yang X. EGCG ameliorates the hypoxia-induced apoptosis and osteogenic differentiation reduction of mesenchymal stem cells via upregulating miR-210. Mol Biol Rep. 2016;43:183–93.
17. Xu J, Huang Z, Lin L, Fu M, Gao Y, Shen Y, Zou Y, Sun A, Qian J, Ge J. miR-210 over-expression enhances mesenchymal stem cell survival in an oxidative stress environment through antioxidation and c-Met pathway activation. Sci China Life Sci. 2014;57:989–97.
18. Shi YF, Liu N, Li YX, Song CL, Song XJ, Zhao Z, Liu B. Insulin protects H9c2 rat cardiomyoblast cells against hydrogen peroxide-induced injury through upregulation of microRNA-210. Free Radic Res. 2015;49:1147–55.
19. Xiao J, Zhou ZC, Chen C, Huo WL, Yin ZX, Weng SP, Chan SM, Yu XQ, He JG. Tumor necrosis factor-alpha gene from mandarin fish, Siniperca chuatsi: Molecular cloning, cytotoxicity analysis and expression profile. Mol Immunol. 2007;44:3615–22.
20. Song P, Xie Z, Guo L, Wang C, Xie W, Wu Y. Human genome-specific real-time PCR method for sensitive detection and reproducible quantitation of human cells in mice. Stem Cell Rev. 2012;8:1155–62.
21. Kim JH, Park SG, Song SY, Kim JK, Sung JH. Reactive oxygen species-responsive miR-210 regulates proliferation and migration of adipose-derived stem cells via PTPN2. Cell Death Dis. 2013;4:e588.
22. Kobayashi CI, Suda T. Regulation of reactive oxygen species in stem cells and cancer stem cells. J Cell Physiol. 2012;227:421–30.
23. Song SY, Chung HM, Sung JH. The pivotal role of VEGF in adipose derived stem cell mediated regeneration. Expert Opin Biol Ther. 2010;10:1529–37.

24. Bhatia SN, Underhill GH, Zaret KS, Fox IJ. Cell and tissue engineering for liver disease. Sci Transl Med. 2014;6: 245sr2.
25. Russo FP, Parola M. Stem and progenitor cells in liver regeneration and repair. Cytotherapy 2011;13:135–44.
26. Chang W, Song BW, Moon JY, Cha MJ, Ham O, Lee SY, Choi E, Choi E, Hwang KC. Anti-death strategies against oxidative stress in grafted mesenchymal stem cells. Histol Histopathol. 2013;28:1529–36.
27. Chen YT, Chiang HJ, Chen CH, Sung PH, Lee FY, Tsai TH, Chang CL, Chen HH, Sun CK, Leu S, Chang HW, Yang CC, Yip HK. Melatonin treatment further improves adipose-derived mesenchymal stem cell therapy for acute interstitial cystitis in rat. J Pineal Res. 2014;57:248–61.
28. Yip HK, Chang YC, Wallace CG, Chang LT, Tsai TH, Chen YL, Chang HW, Leu S, Zhen YY, Tsai CY, Yeh KH, Sun CK, Yen CH. Melatonin treatment improves adipose-derived mesenchymal stem cell therapy for acute lung ischemia-reperfusion injury. J Pineal Res. 2013;54:207–21.
29. Sadelain M. The need for genetically engineering therapeutic pluripotent stem cells. Mol Ther. 2010;18:2039.
30. Karioti A, Bergonzi MC, Vincieri FF, Bilia AR. Validated method for the analysis of goji berry, a rich source of zeaxanthin dipalmitate. J Agric Food Chem. 2014;62:12529–35.
31. Pervaiz S, Taneja R, Ghaffari S. Oxidative stress regulation of stem and progenitor cells. Antioxid Redox Signal. 2009;11:2777–89.